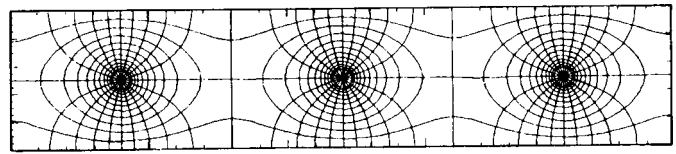
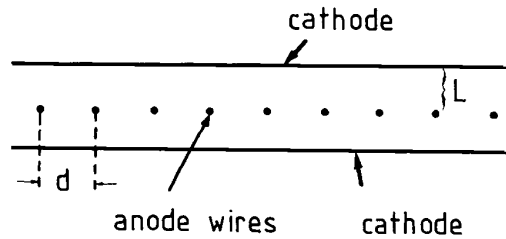


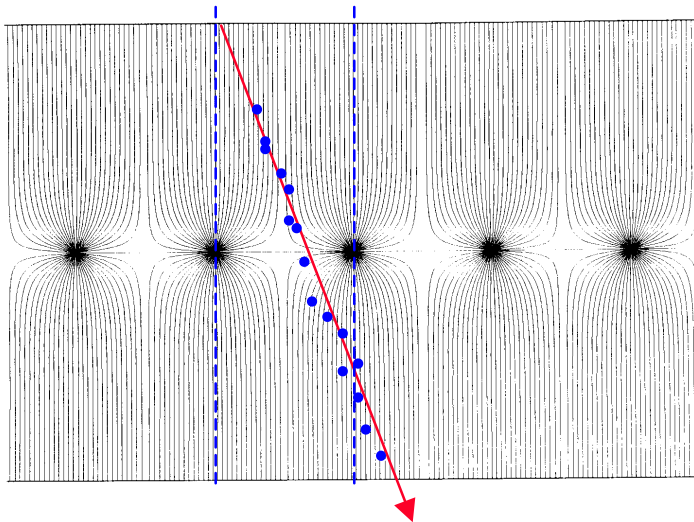
Multi wire proportional chamber (MWPC)

(G. Charpak et al. 1968, Nobel prize 1992)



field lines and equipotentials around anode wires

Capacitive coupling of non-screened parallel wires?
 Negative signals on all wires? Compensated by
 positive signal induction from ion avalanche.



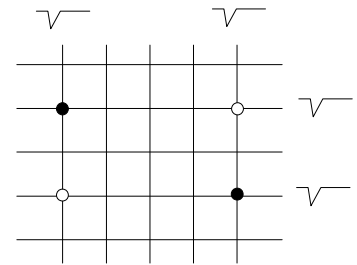
Typical parameters:
 $L=5\text{mm}$, $d=1\text{mm}$,
 $a_{\text{wire}}=20\text{mm}$.

Normally digital readout:
 spatial resolution limited to $s_x \approx \frac{d}{\sqrt{12}}$ ($d=1\text{mm}$,
 $\sigma_x=300\text{mm}$)

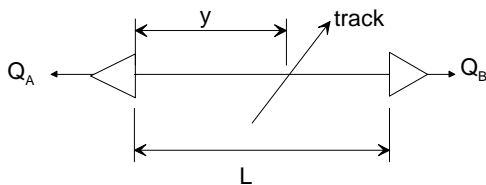
Address of fired wire(s) give only 1-dimensional
 information. Secondary coordinate

Secondary coordinate

- ◆ **Crossed wire planes. Ghost hits.**
Restricted to low multiplicities. Also stereo planes (crossing under small angle).

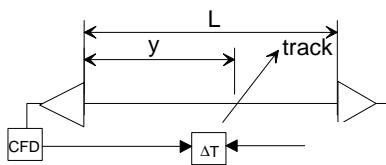


- ◆ **Charge division. Resistive wires (Carbon, 2kΩ/m).**



$$\frac{y}{L} = \frac{Q_B}{Q_A + Q_B} \quad s\left(\frac{y}{L}\right) \text{ up to } 0.4\%$$

- ◆ **Timing difference (DELPHI Outer detector, OPAL vertex detector)**

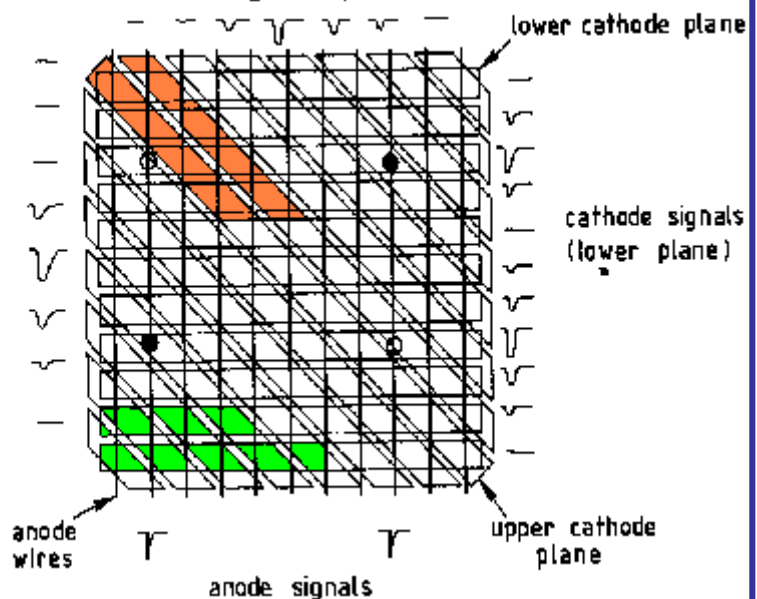


$$s(\Delta T) = 100 \text{ ps}$$

$$\rightarrow s(y) \approx 4 \text{ cm} \quad (\text{OPAL})$$

cathode signals (upper plane)

- ◆ **1 wire plane**
+ 2 segmented cathode planes

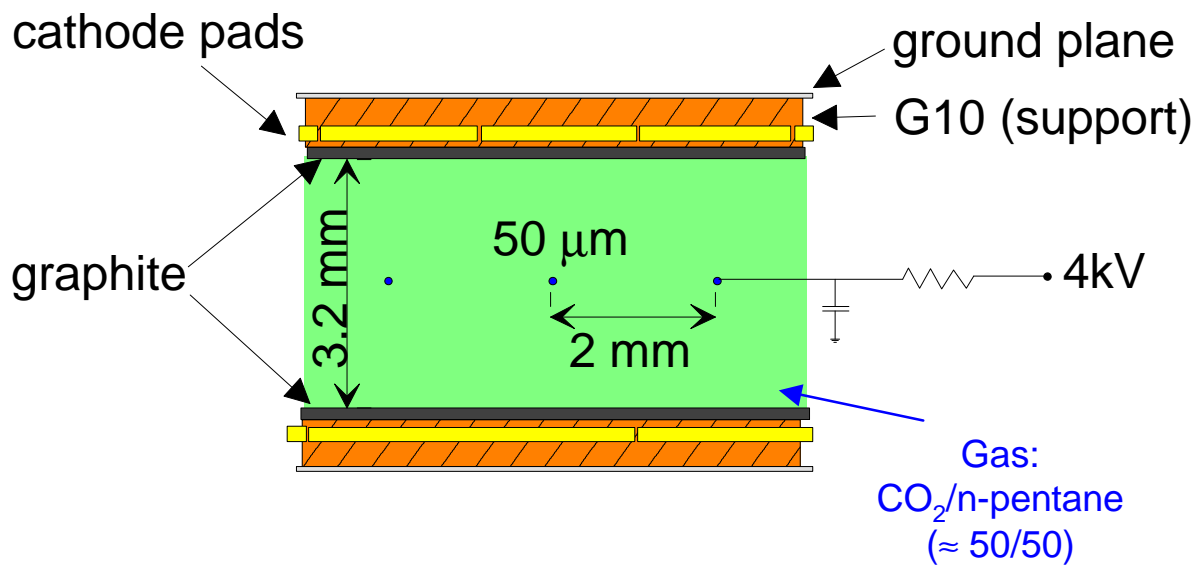


Analog readout of cathode planes.

$$\rightarrow \sigma \approx 100 \mu\text{m}$$

Some 'derivatives'

◆ Thin gap chambers (TGC)



Operation in **saturated mode**. Signal amplitude limited by the resistivity of the graphite layer ($\approx 40\text{k}\Omega/\square$).

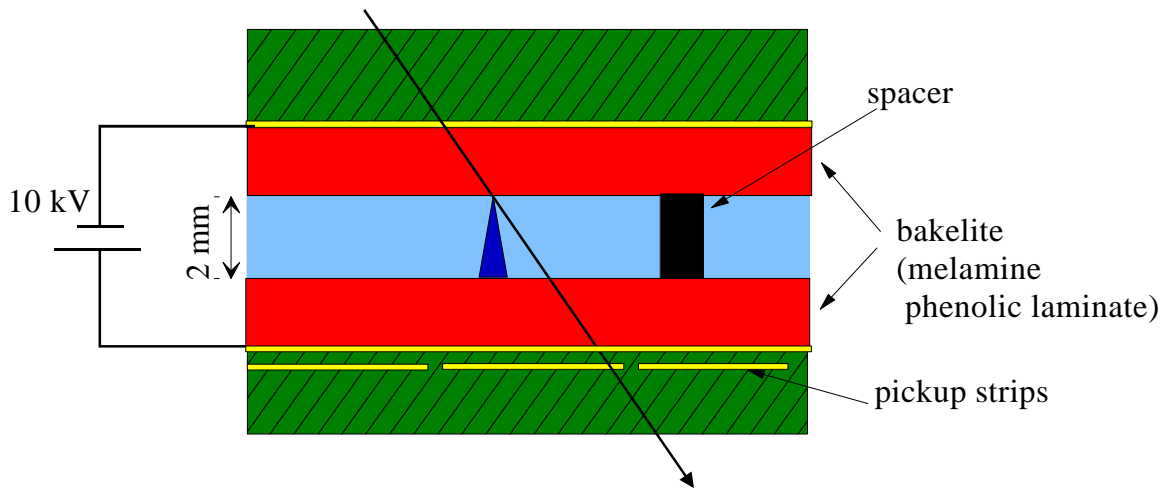
Fast (2 ns risetime), large signals (gain 10^6), robust

Application: OPAL pole tip hadron calorimeter.

G. Mikenberg, NIM A 265 (1988) 223

ATLAS muon endcap trigger, Y.Arai et al. NIM A 367 (1995) 398

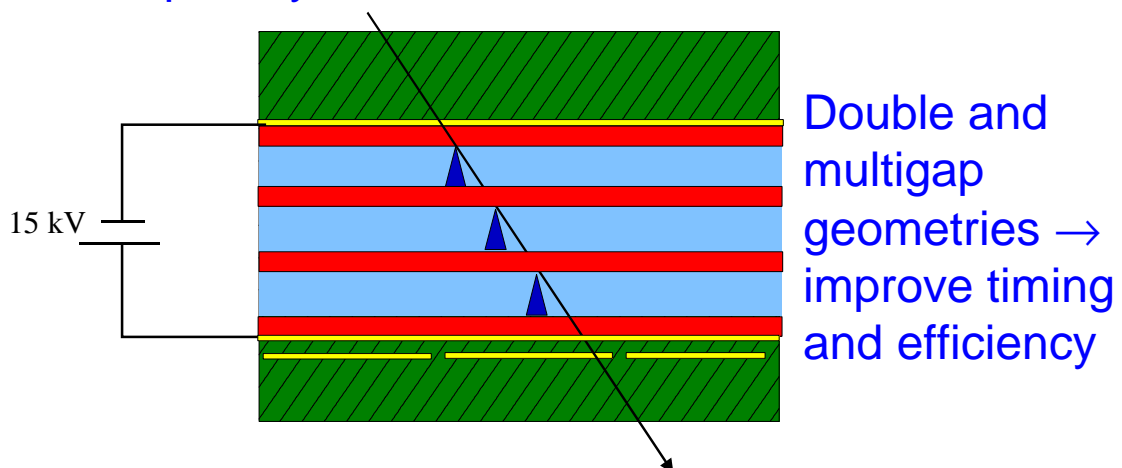
◆ Resistive plate chambers (RPC) No wires !



Gas: $C_2F_4H_2$, (C_2F_5H) + few % isobutane

(ATLAS, A. Di Ciaccio, NIM A 384 (1996) 222)

Time dispersion $\approx 1..2$ ns \rightarrow suited as trigger chamber
 Rate capability ≈ 1 kHz / cm²

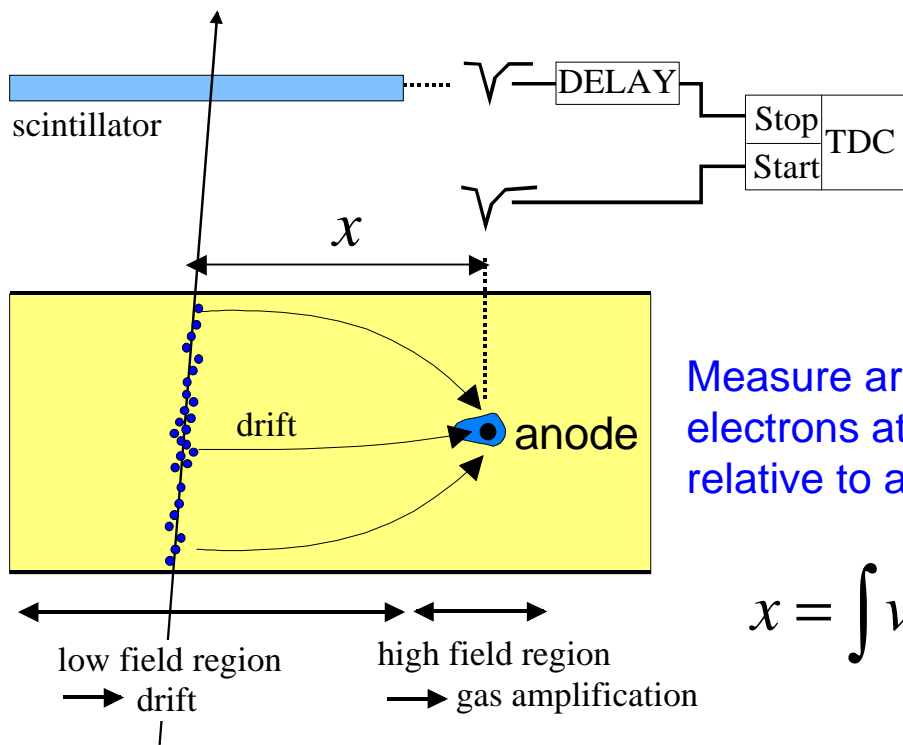


Double and multigap geometries \rightarrow improve timing and efficiency

Problem: Operation close to streamer mode.

Drift chambers

(First studies: T. Bressani, G. Charpak, D. Rahm, C. Zupancic, 1969
 First operation drift chamber: A.H. Walenta, J. Heintze, B. Schürlein, NIM 92 (1971) 373)



Measure arrival time of electrons at sense wire relative to a time t_0 .

$$x = \int v_D(t) dt$$

What happens during the drift towards the anode wire ?

- 👉 Diffusion ?
- 👉 Drift velocity ?

Drift and diffusion in gases

No external fields:

Electrons and ions will lose their energy due to collisions with the gas atoms → thermalization

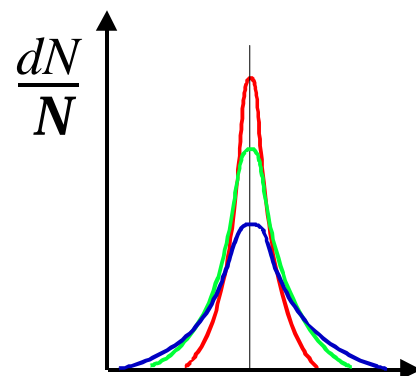
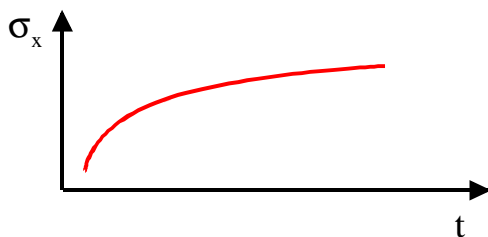
$$e = \frac{3}{2} kT \approx 40 \text{ meV}$$

Undergoing multiple collisions, an originally localized ensemble of charges will diffuse

$$\frac{dN}{N} = \frac{1}{\sqrt{4pDt}} e^{-(x^2/4Dt)} dx$$

D : diffusion coefficient

$$s_x(t) = \sqrt{2Dt} \quad \text{or} \quad D = \frac{s_x^2(t)}{2t}$$

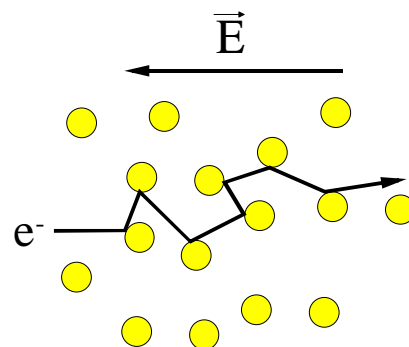


External electric field:

“stop and go” traffic due to scattering from gas atoms

Ⓡ drift

$$\vec{v}_D = m\vec{E} \quad m = \frac{e\tau}{m} \text{ (mobility)}$$



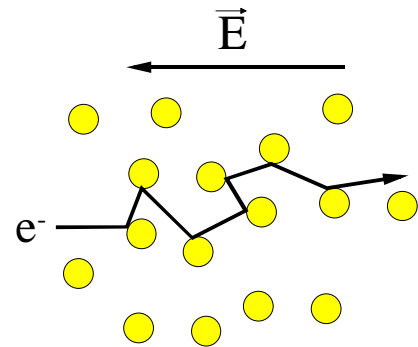
in the equilibrium ...

$$\frac{x}{v_D t} I_e e = e E x$$

I_e : fractional energy loss / collision

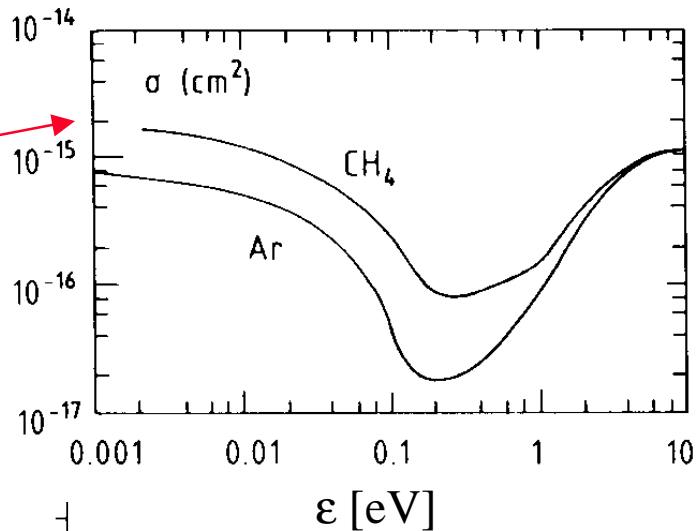
$$t = \frac{1}{N S v} \quad v: \text{instantaneous velocity}$$

$$\rightarrow v_D^2 = \frac{e E}{m N S} \sqrt{\frac{I}{2}}$$

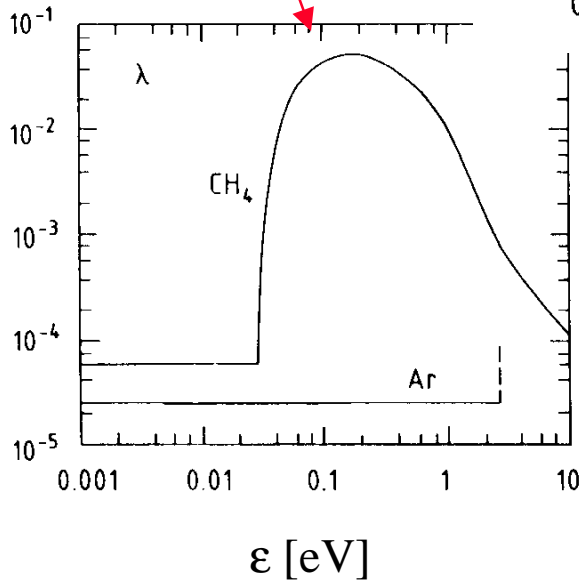


$\sigma = \sigma(\epsilon) !$

$\lambda = \lambda(\epsilon) !$



(B. Schmidt, thesis, unpublished, 1986)



Typical electron drift velocity: **5 cm/ms**

Ion drift velocities: ca. 1000 times smaller

In the presence of electric and magnetic fields, drift and diffusion are driven by $\vec{E} \times \vec{B}$ effects

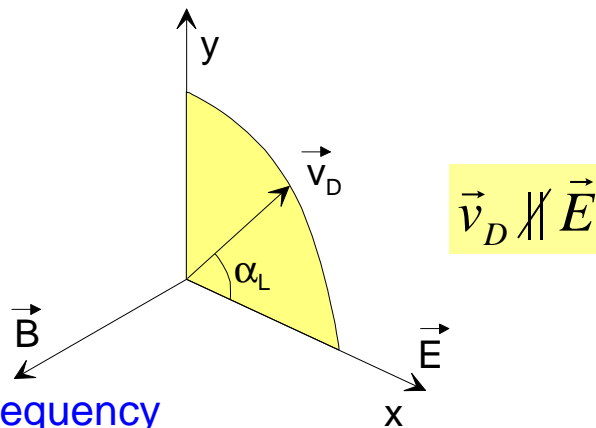
Look at 2 special cases:

Special case: $\vec{E} \perp \vec{B}$

$$\tan \alpha_L = \omega t$$

α_L : Lorentz angle

$$\omega = \frac{e\vec{B}}{m} \quad \text{cyclotron frequency}$$



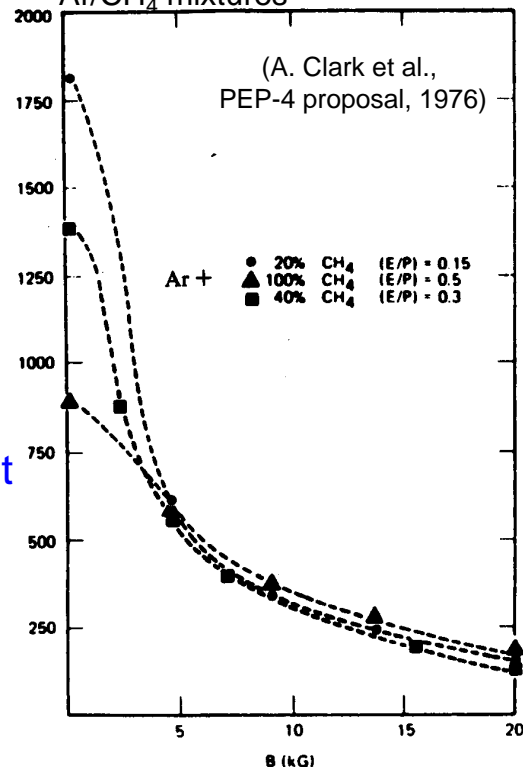
Special case: $\vec{E} \parallel \vec{B}$

The longitudinal diffusion (along B-field) is unchanged. In the transverse projection the electrons are forced on circle segments with the radius v_T/ω . The transverse diffusion coefficient appears reduced

$$D_T(B) = \frac{D_0}{1 + \omega^2 t^2}$$

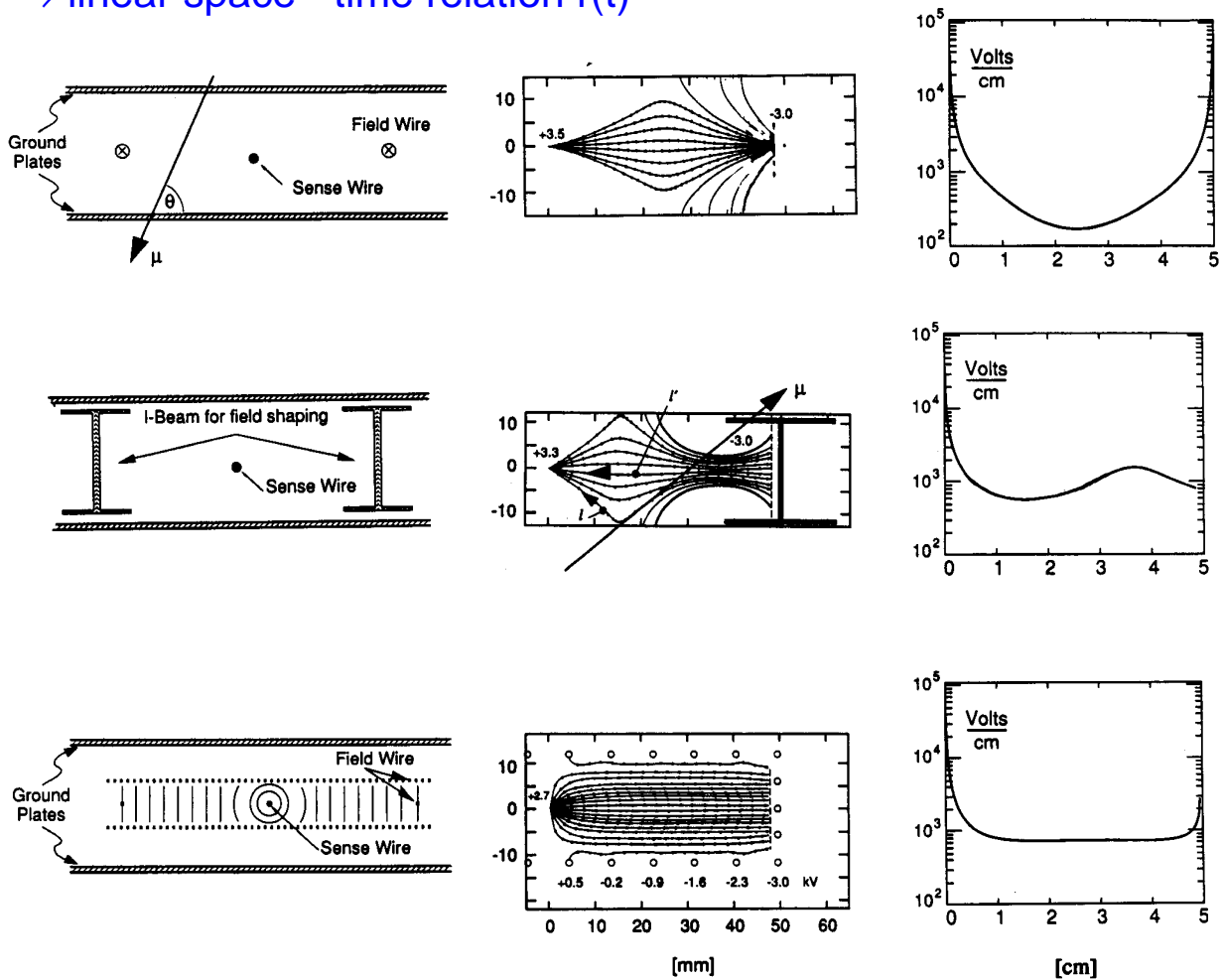
Very useful... see later !

Transverse diffusion σ (μm) for a drift of 15 cm in different Ar/CH₄ mixtures



Some planar drift chamber designs

Optimize geometry → constant E-field
 Choose drift gases with little dependence $v_D(E)$
 → linear space - time relation $r(t)$

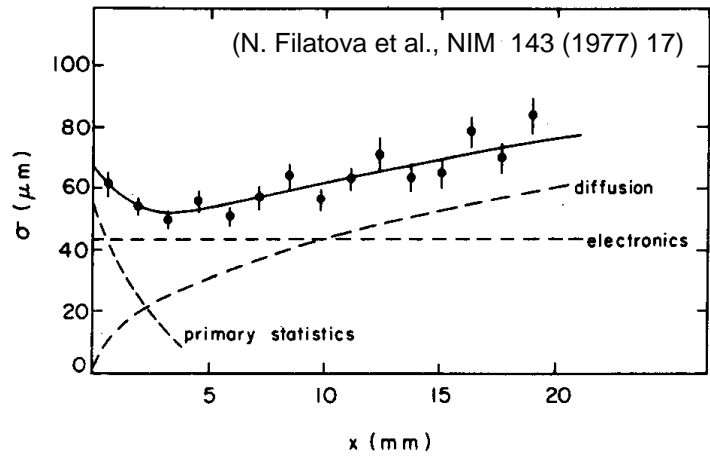


(U. Becker, in: Instrumentation in High Energy Physics, World Scientific)

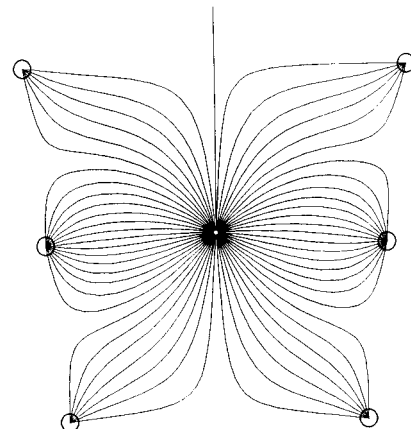
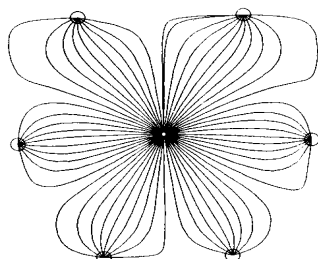
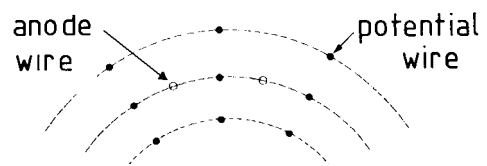
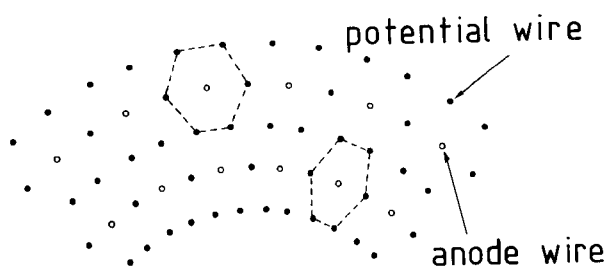
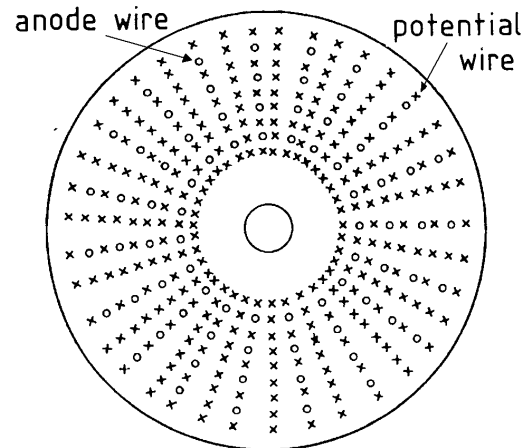
The spatial resolution is not limited by the cell size
 → less wires, less electronics,
 less support structure than in MWPC.

Resolution determined by

- diffusion,
- path fluctuations,
- electronics
- primary ionization statistics

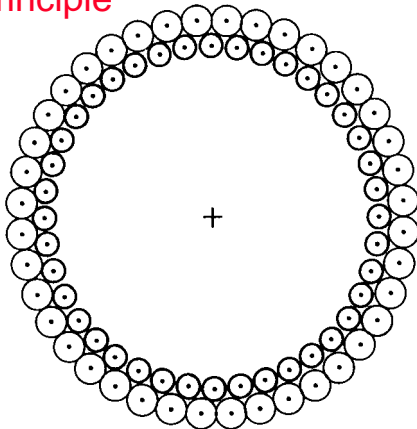


Various geometries of cylindrical drift chambers



Straw tubes: Thin cylindrical cathode, 1 anode wire

principle

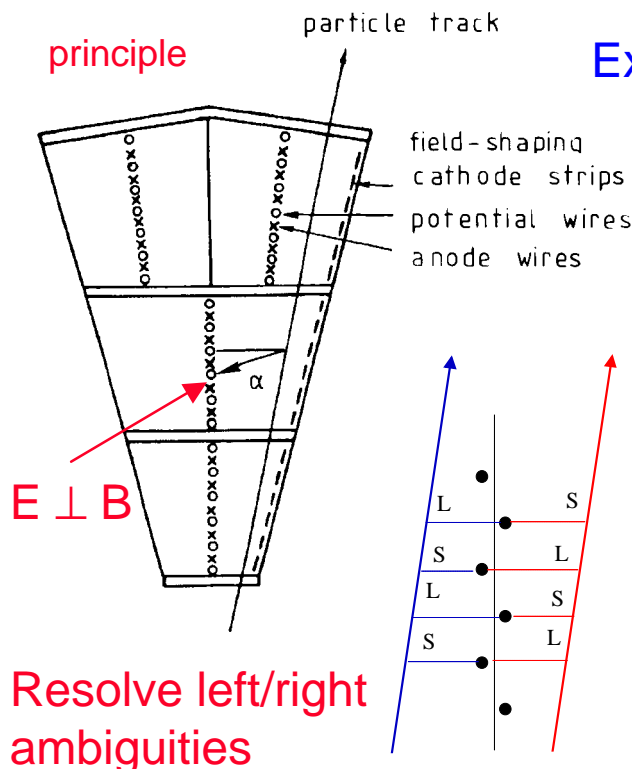


Example: DELPHI Inner detector

5 layers with 192 tubes each
 tube \varnothing 0.9 cm, 2 m long,
 wall thickness 30 μm (Al coated polyester)
 wire \varnothing 40 μm
 Intrinsic resolution ca. 50 μm

Jet chambers: Optimized for maximum number of measurements in radial direction

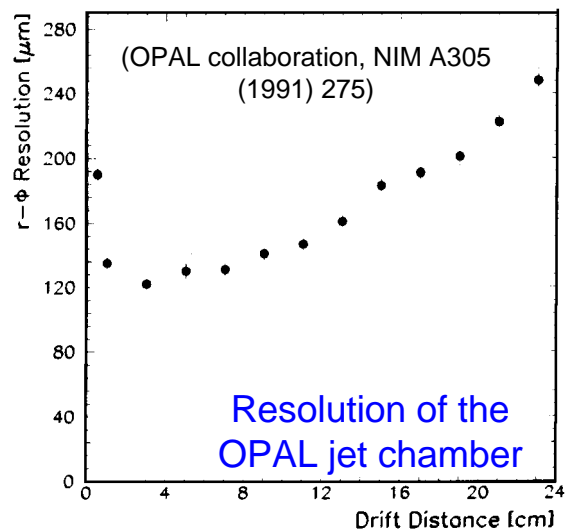
principle



Example: OPAL Jet chamber

$\varnothing=3.7\text{m}$, $L=4\text{m}$, 24 sectors à
 159 sense wires ($\pm 100 \mu\text{m}$
 staggered). $3 \text{ cm} < l_{\text{drift}} < 25 \text{ cm}$

Resolve left/right ambiguities



Time Projection Chamber [®] full 3-D track reconstruction

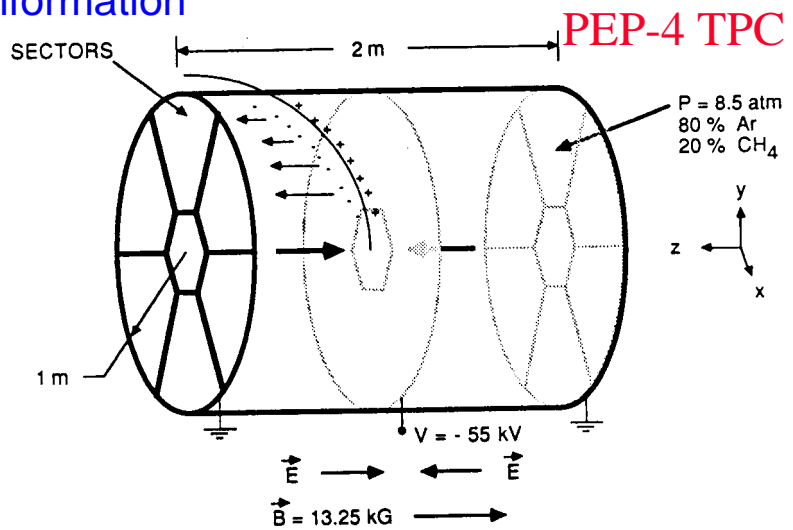
- ◆ x-y from wires and segmented cathode of MWPC
- ◆ z from drift time
- ◆ in addition dE/dx information

Diffusion significantly reduced by B-field.

Requires precise knowledge of $v_D \rightarrow$ LASER calibration + ρ, T corrections

Drift over long distances \rightarrow very good gas quality required

Space charge problem from positive ions, drifting back to midwall \rightarrow gating

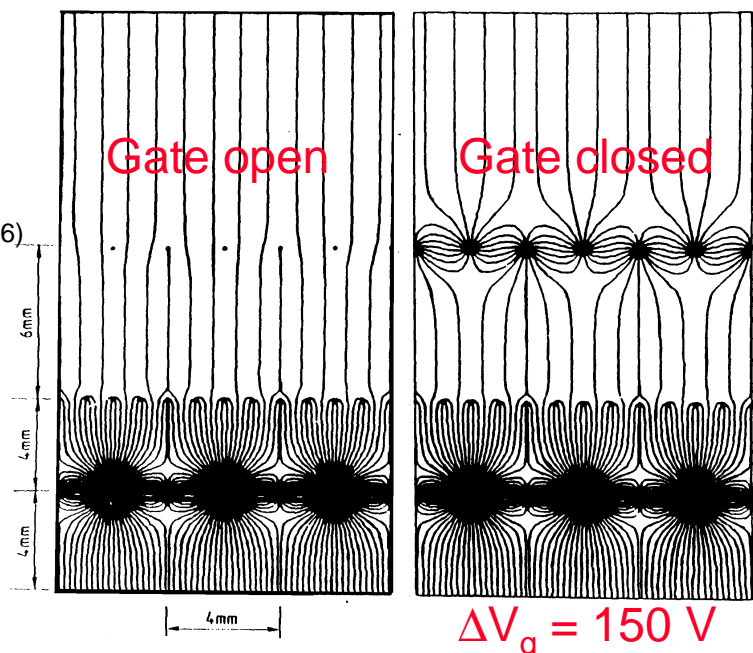


ALEPH TPC

(ALEPH coll., NIM A 294 (1990) 121, W. Atwood et. Al, NIM A 306 (1991) 446)

\varnothing 3.6M, L=4.4 m

$\sigma_{R\phi} = 173 \mu\text{m}$
 $\sigma_z = 740 \mu\text{m}$
 (isolated leptons)



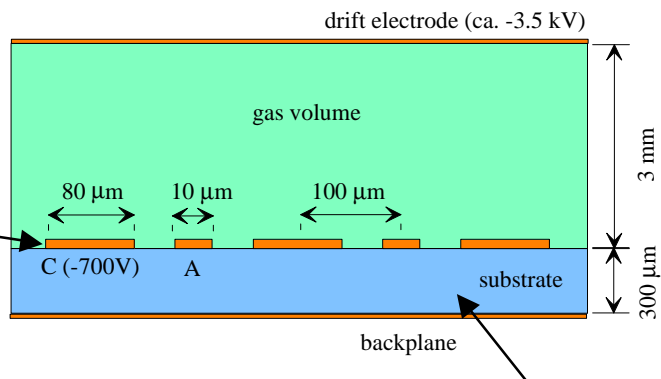
Faster and more precision ? → smaller structures

◆ Microstrip gas chambers

(A. Oed, NIM A 263 (1988) 352)

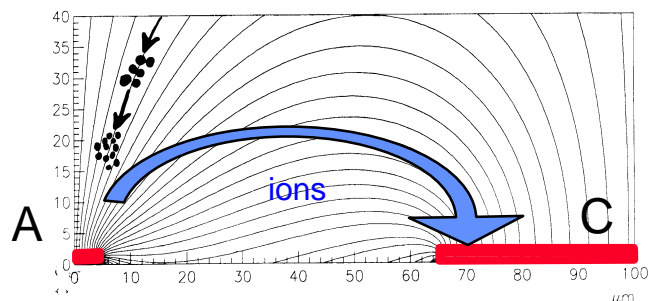
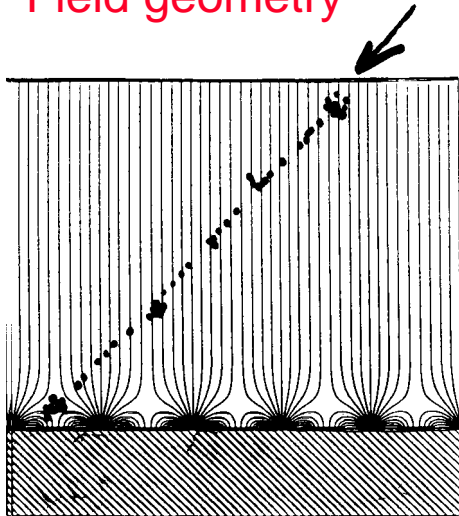
geometry and typical dimensions
(former CMS standard)

Gold strips
+ Cr underlayer



Glass DESAG AF45 + S8900
semiconducting glass coating,
 $\rho=10^{16} \Omega/\square$

Field geometry



Fast ion evacuation → high rate capability
 $\approx 10^6 /(\text{mm}^2 \cdot \text{s})$

Gas: Ar-DME, Ne-DME (1:2), Lorentz angle 14° at 4T,
Gain $\leq 10^4$

CMS

Passivation: non-conductive protection of cathode edges

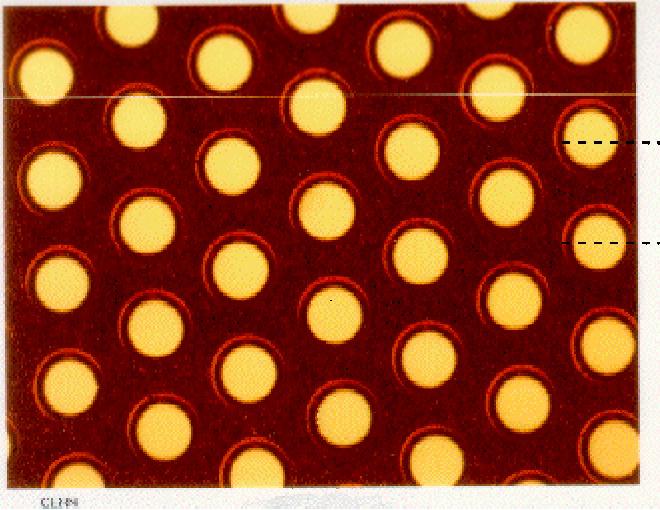
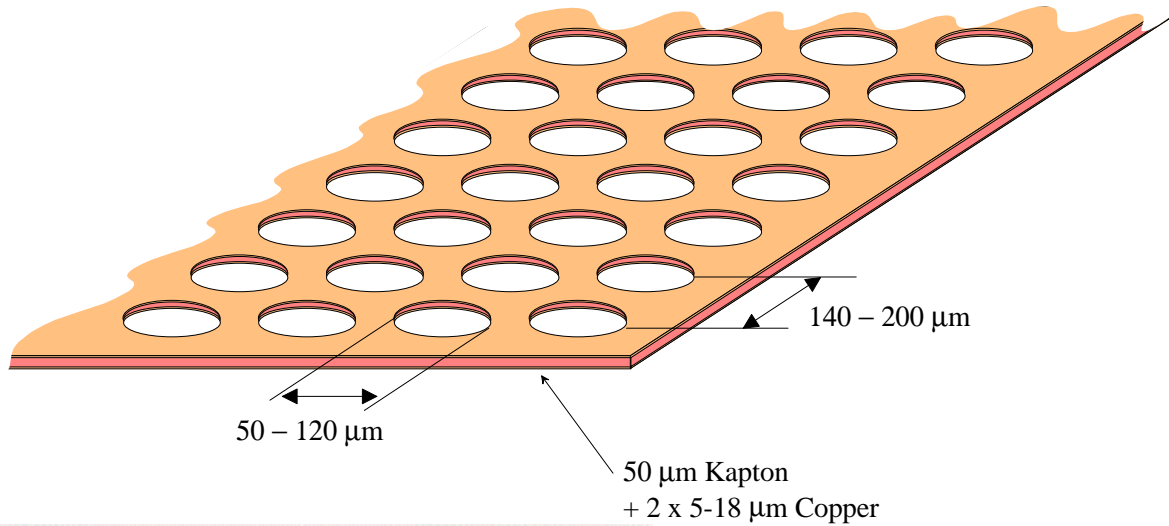
Resolution: $\approx 30..40 \mu\text{m}$

Aging: Seems to be under control.

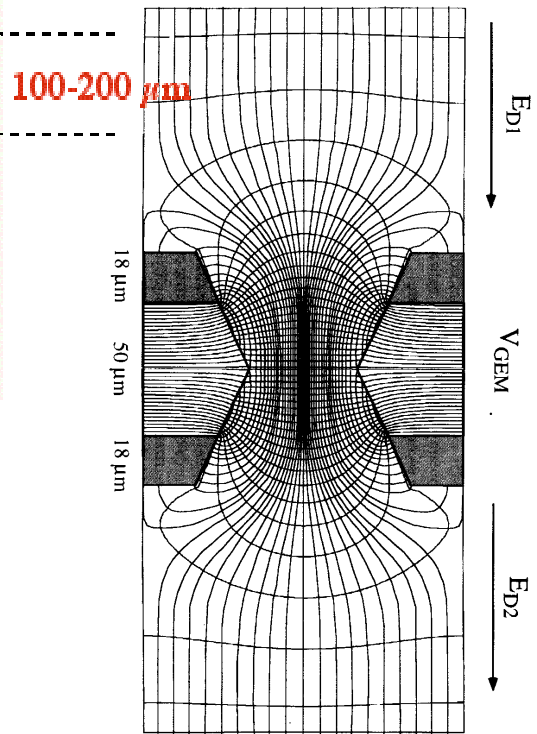
10 years LHC operation $\approx 100 \text{ mC/cm}$

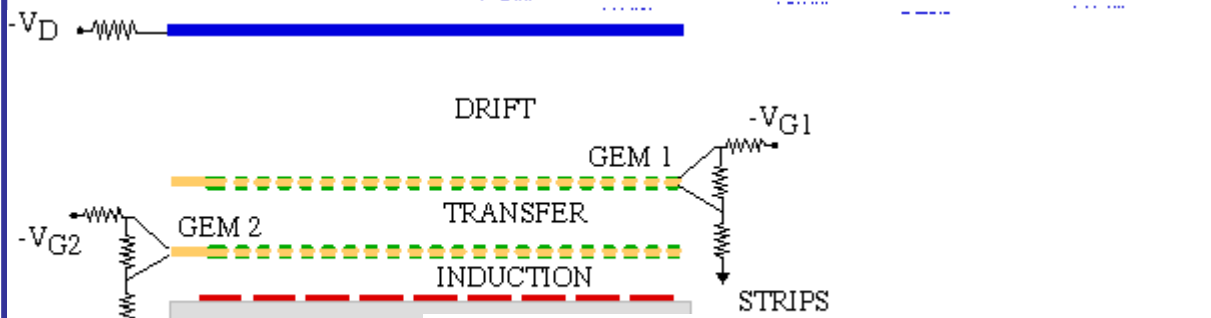
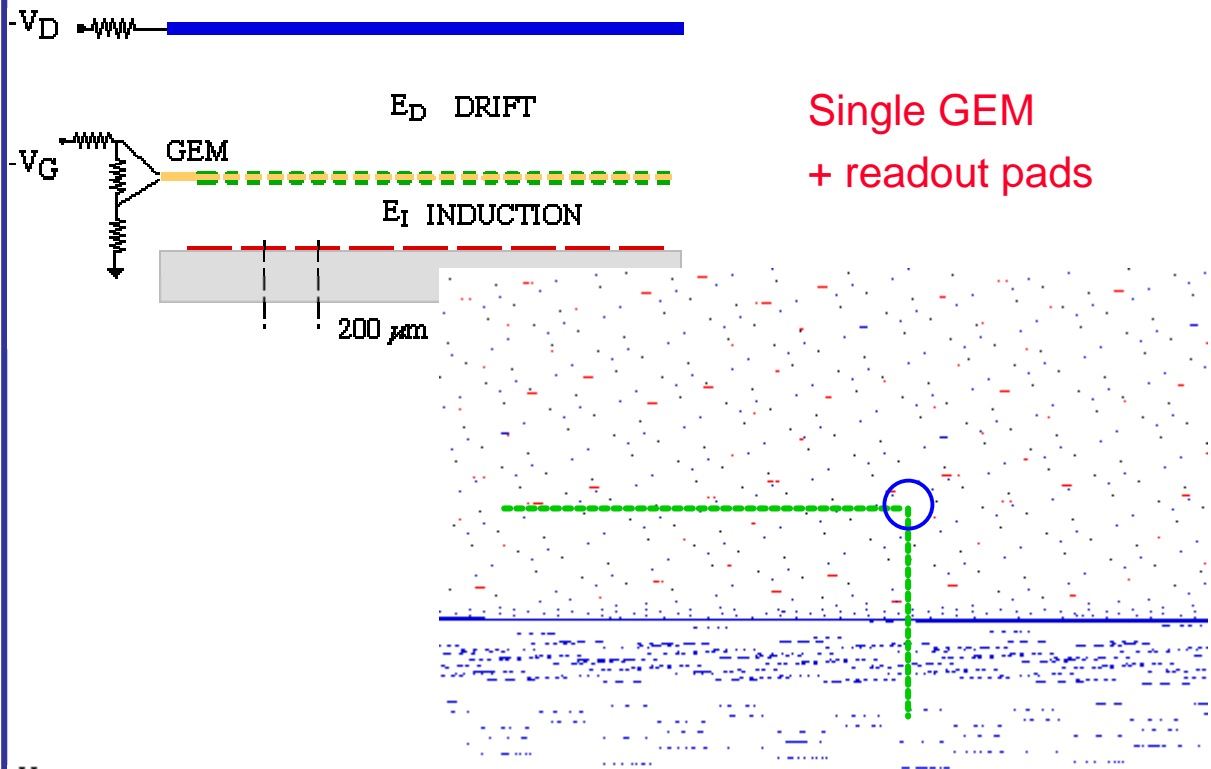
◆ GEM: The Gas Electron Multiplier

(R. Bouclier et al., NIM A 396 (1997) 50)



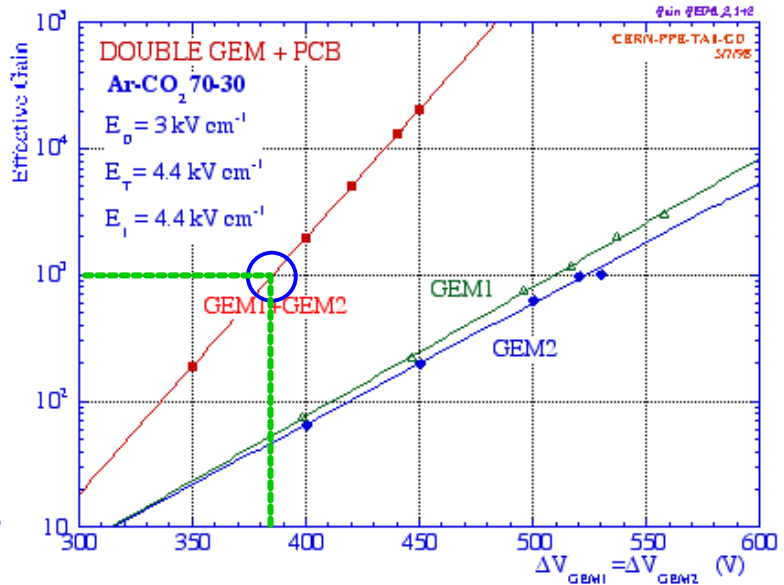
Micro photo of a GEM foil





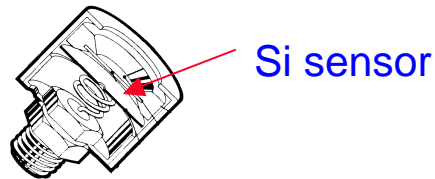
Double GEM + readout pads

- Same gain at lower voltage
- Less discharges

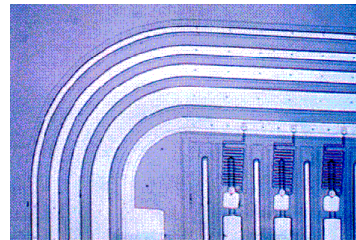


Silicon detectors

Solid state detectors have a long tradition for energy measurements (Si, Ge, Ge(Li)).



Here we are interested in their use as precision trackers !

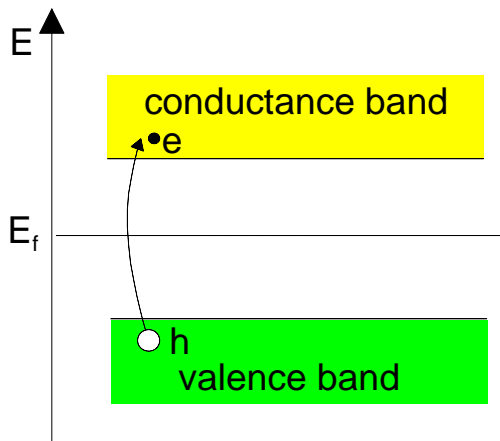


ATLAS
SCT

Some characteristic numbers for silicon

- 👉 Band gap: $E_g = 1.12$ V.
- 👉 $E(e^-$ -hole pair) = 3.6 eV, (≈ 30 eV for gas detectors).
- 👉 High specific density (2.33 g/cm³) $\rightarrow \Delta E$ /track length for M.I.P.'s.: 390 eV/ μ m ≈ 108 e-h/ μ m (average)
- 👉 High mobility: $\mu_e = 1450$ cm²/Vs, $\mu_h = 450$ cm²/Vs
- 👉 Detector production by microelectronic techniques \rightarrow small dimensions \rightarrow fast charge collection (< 10 ns).
- 👉 Rigidity of silicon allows thin self supporting structures.
Typical thickness 300 μ m $\rightarrow \approx 3.2 \cdot 10^4$ e-h (average)
- 👉 But: No charge multiplication mechanism!

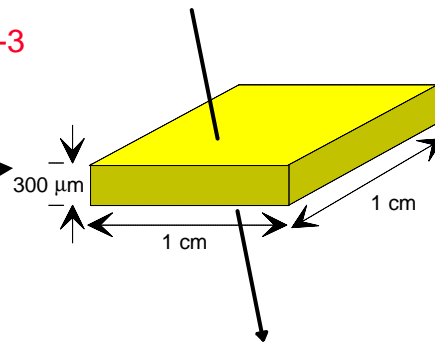
How to obtain a signal ?



In a pure intrinsic (undoped) material the electron density n and hole density p are equal. $n = p = n_i$

For Silicon: $n_i \approx 1.45 \cdot 10^{10} \text{ cm}^{-3}$

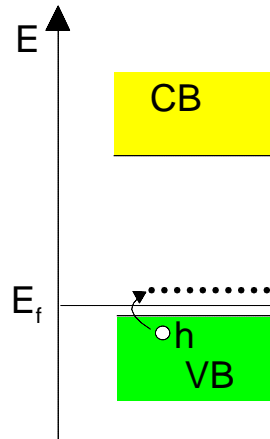
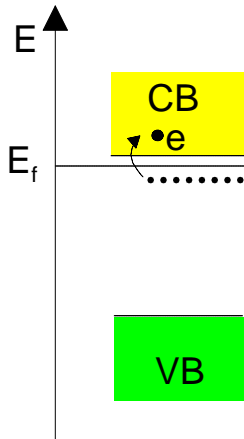
In this volume we have $4.5 \cdot 10^8$ free charge carriers, but only $3.2 \cdot 10^4$ e-h pairs produced by a M.I.P.



→ Reduce number of free charge carriers, i.e. deplete the detector

Most detectors make use of reverse biased p-n junctions

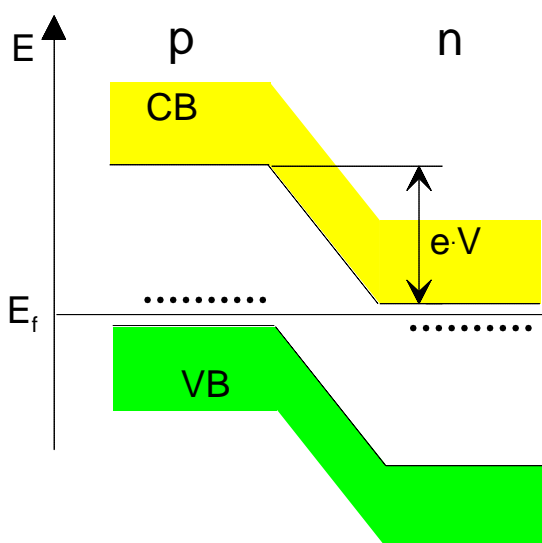
Doping



n-type: Add elements from Vth group, **donors**, e.g. As. Electrons are the majority carriers.

p-type: Add elements from IIIrd group, **acceptors**, e.g. B. Holes are the majority carriers.

	detector grade	electronics grade
doping concentration	$10^{12} \text{ cm}^{-3} \text{ (n)} - 10^{15} \text{ cm}^{-3} \text{ (p}^+)$	$10^{17(18)} \text{ cm}^{-3}$
resistivity	$\approx 5 \text{ k}\Omega\cdot\text{cm}$	$\approx 1 \text{ }\Omega\cdot\text{cm}$

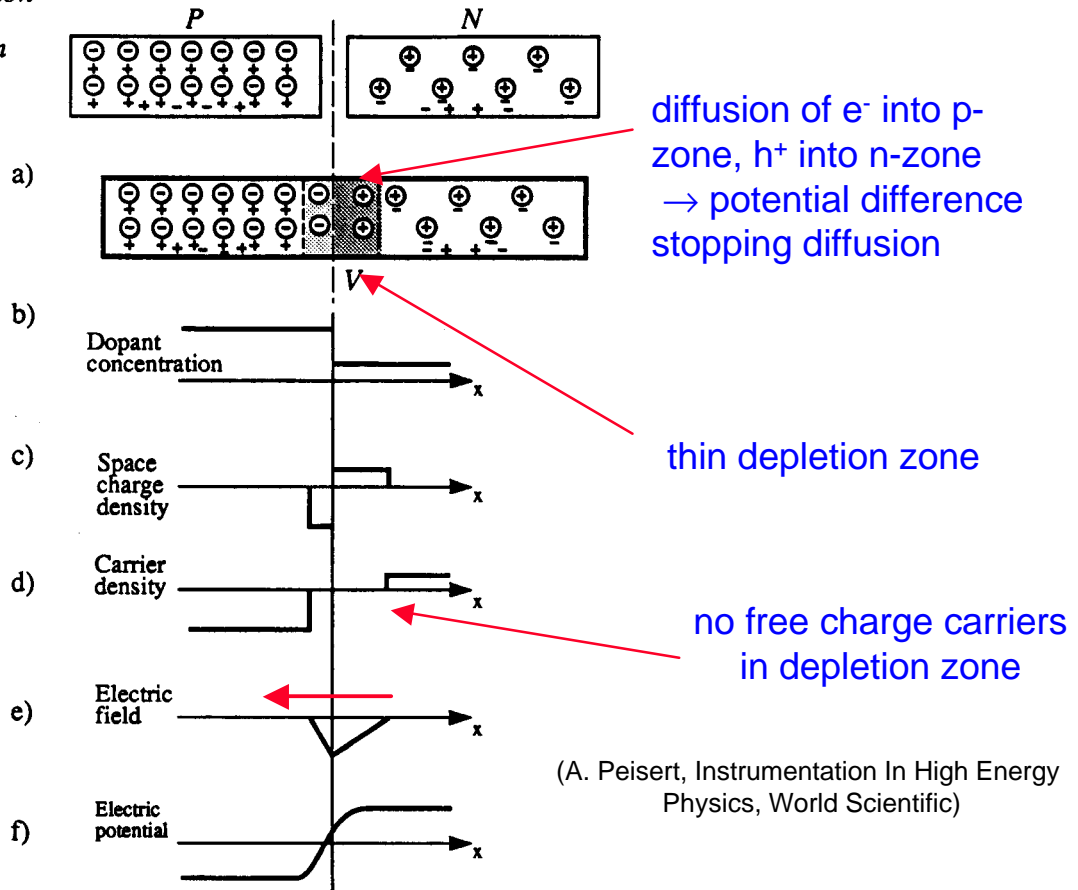


pn junction

There must be a single Fermi level !
Deformation of band structure \rightarrow **potential difference.**

⊖ Acceptor ion
 ⊕ Donor ion
 + Hole
 - Electron

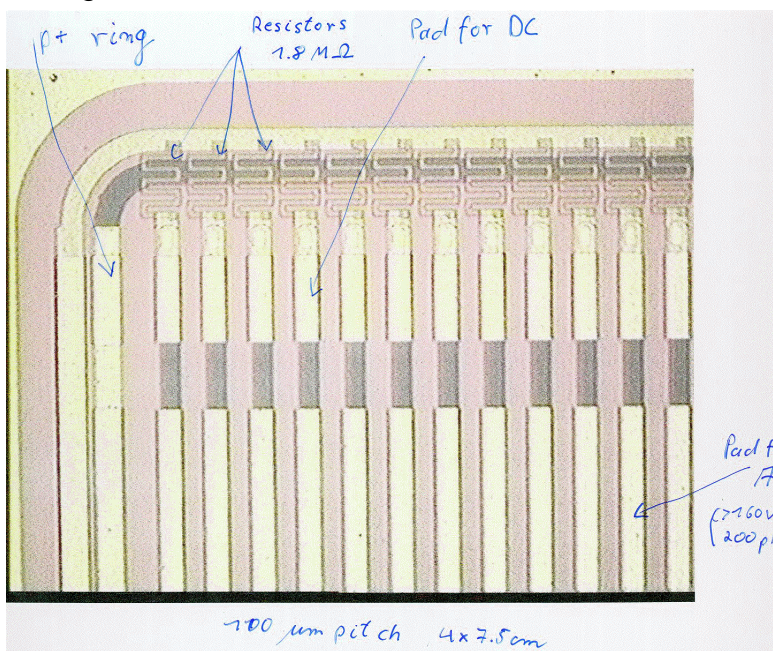
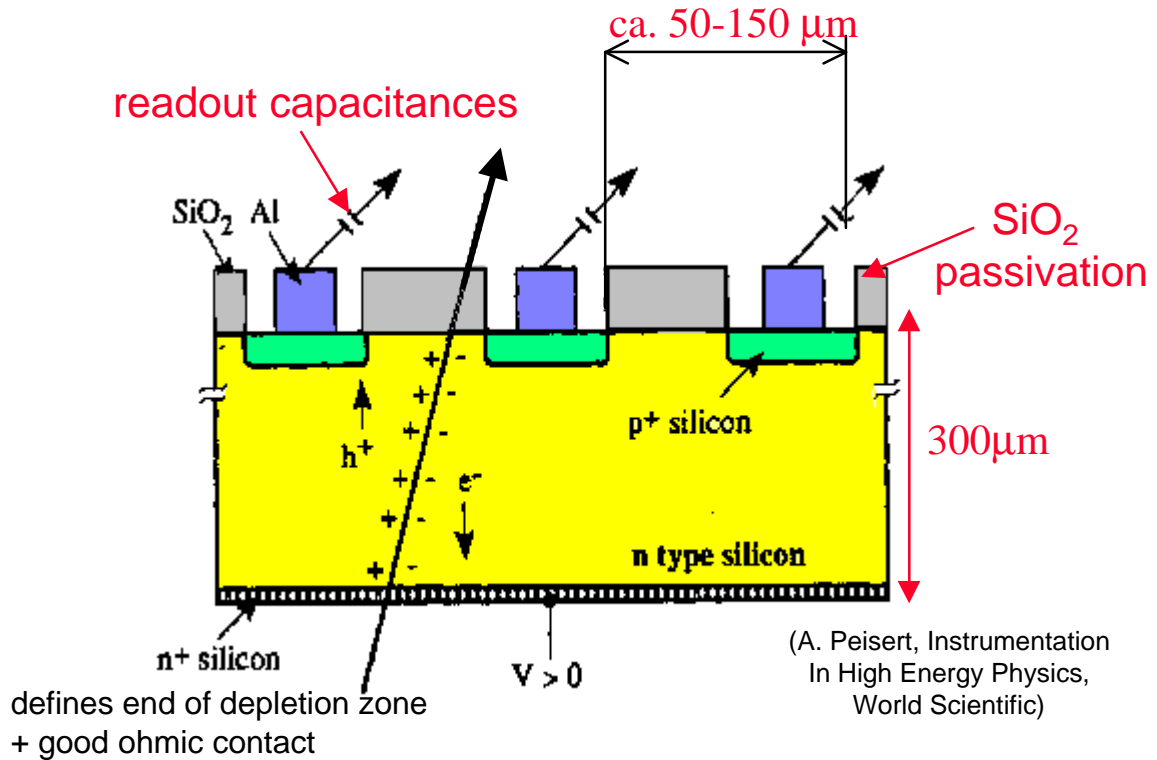
THE PN JUNCTION



- Application of a **reverse bias voltage** (about 100V) → the thin depletion zone gets extended over the full junction → **fully depleted detector**.
- **Energy deposition in the depleted zone**, due to traversing charged particles or photons (X-rays), creates **free e^- -hole pairs**.
- Under the influence of the E-field, the electrons drift towards the n-side, the holes towards the p-side → **detectable current**.

Spatial information by segmenting
the p doped layer →
single sided microstrip detector.

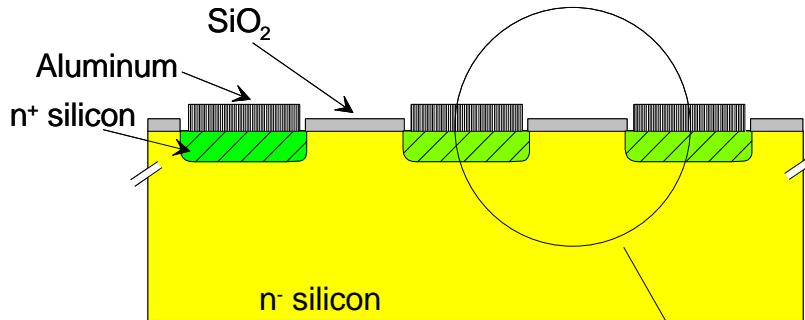
Schematically !



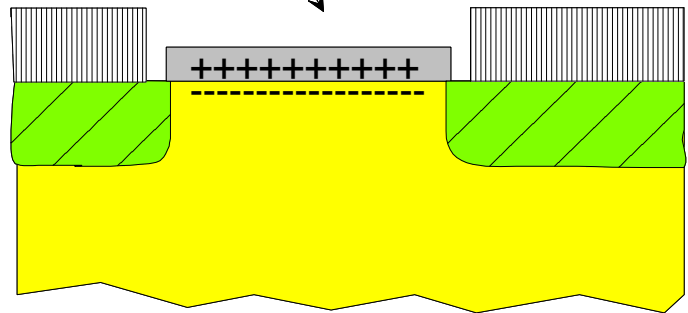
ALICE: Single sided
micro strip prototype

Segmenting also the n doped layer → Double sided microstrip detector.

But:

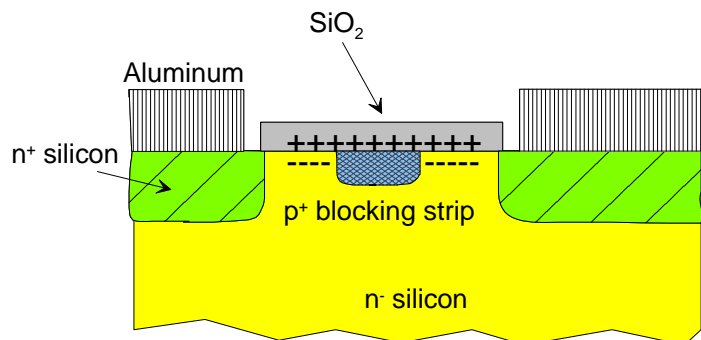


Positive charges in SiO_2 attract e^- in n- layer. Short circuits between n+ strips.

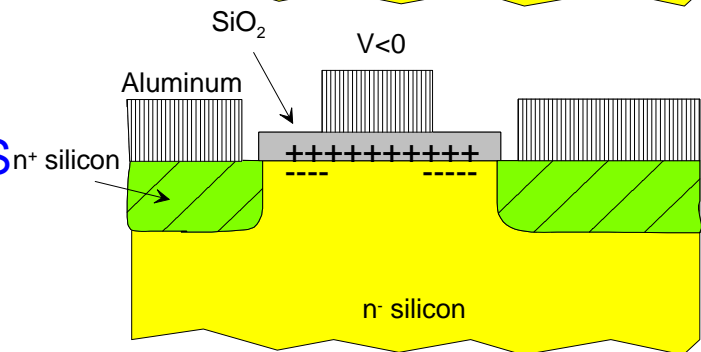


Two solutions:

Add p+ doped blocking strips

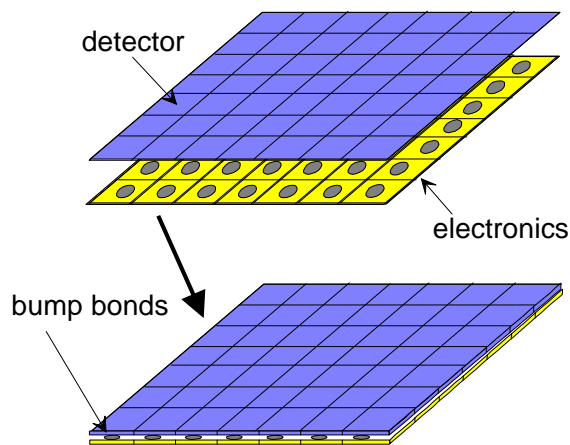


Add Aluminum layer on top of SiO_2
 Negative biased MOS (metal oxide semiconductor) structure repelling e^-



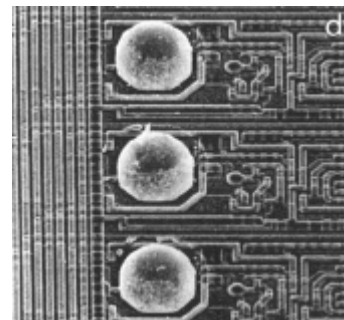
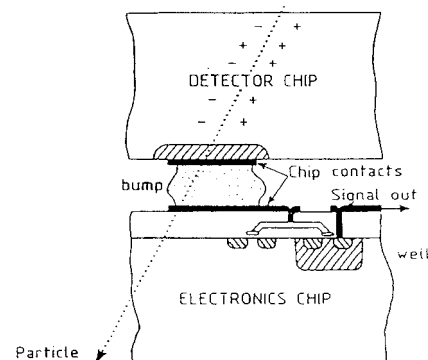
◆ Silicon pixel detectors

- Segment silicon to diode matrix
- also readout electronic with same geometry
- connection by bump bonding techniques



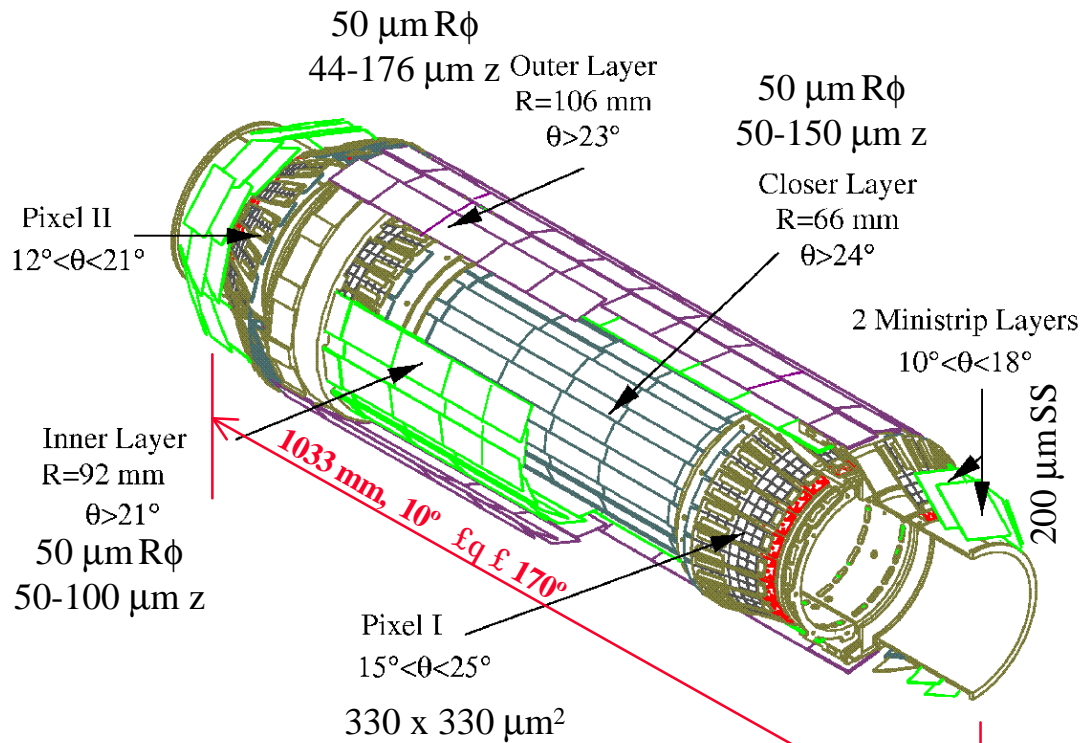
RD 19, E. Heijne et al., NIM A 384 (1994) 399

Flip-chip technique



- Requires sophisticated readout architecture
- First experiment WA94 (1991), WA97
- OMEGA 3 / LHC1 chip (2048 pixels, $50 \times 500 \mu\text{m}^2$) (CERN ECP/96-03)
- Pixel detectors will be used also in LHC experiments (ATLAS, ALICE, CMS)

◆ The DELPHI micro vertex detector (since 1996)

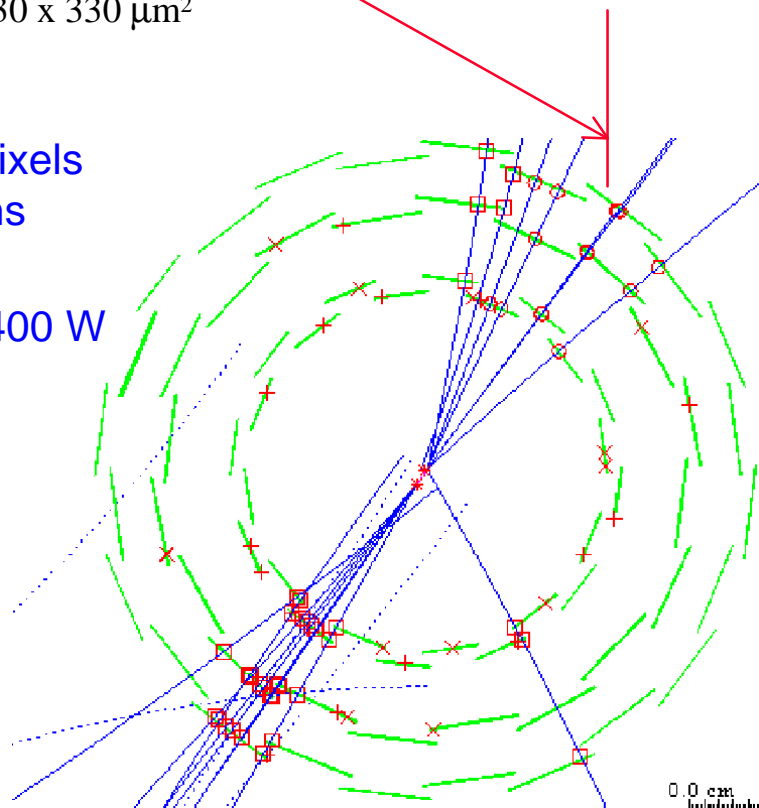


readout channels
 ca. 174 k strips, 1.2 M pixels
 total readout time: 1.6 ms

Total dissipated power 400 W
 → water cooling system

Hit resolution in barrel
 part $\approx 10 \mu\text{m}$
 Impact parameter
 resolution ($r\phi$)

$$28\text{mm} \oplus 71 / \left(p \sin^{\frac{3}{2}} \theta \right)$$



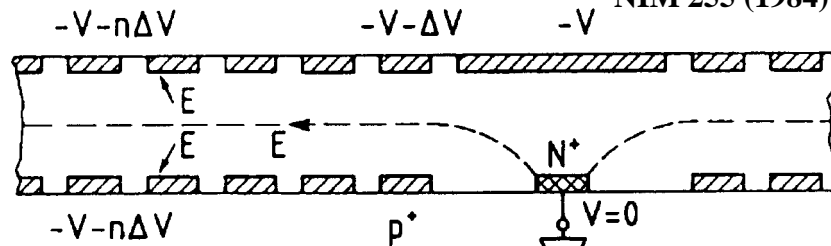
0.0 cm

◆ Silicon drift chamber

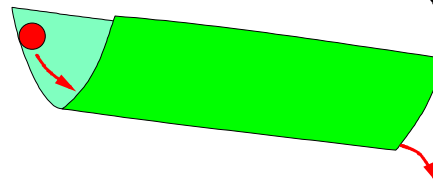
(First proposed by
E. Gatti and P. Rehak,

NIM 255 (1984) 608)

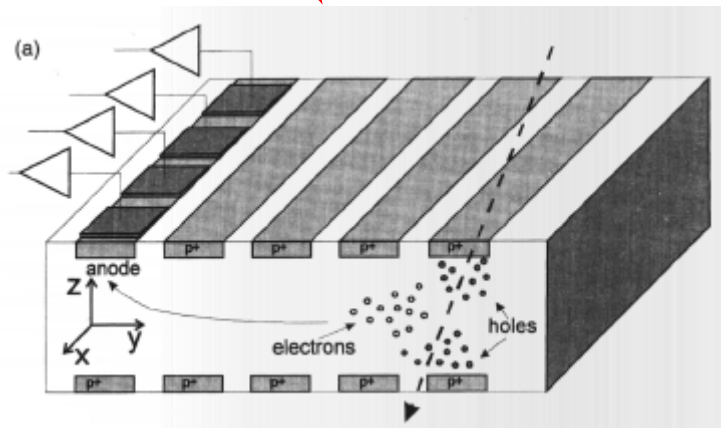
principle:



Define graded potentials on p+ implants.
Measure arrival time at n+ strip

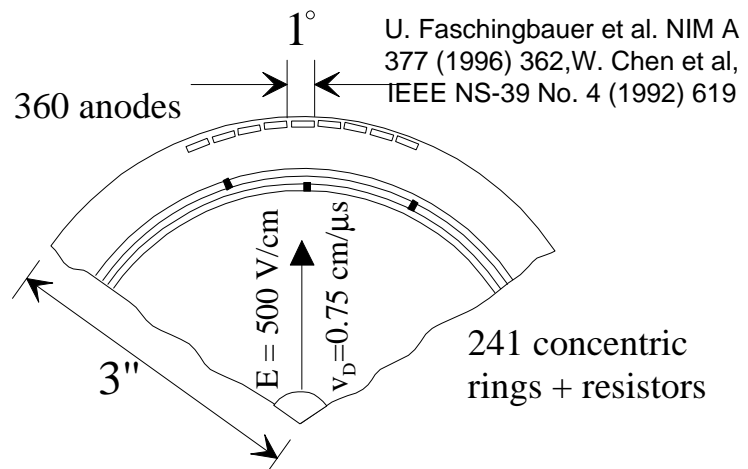


Segmentation of n+ strip into pads
→ 2-D readout



CERES (NA45):
doublet of 3" radial
Si drift chambers

Intrinsic resolution:
 $\sigma_R \approx 20 \mu\text{m}$, $\sigma_\phi \approx 2 \text{ mrad}$



The whole charge is collected at one small collecting electrode. Small capacity (100 fF) → low noise.

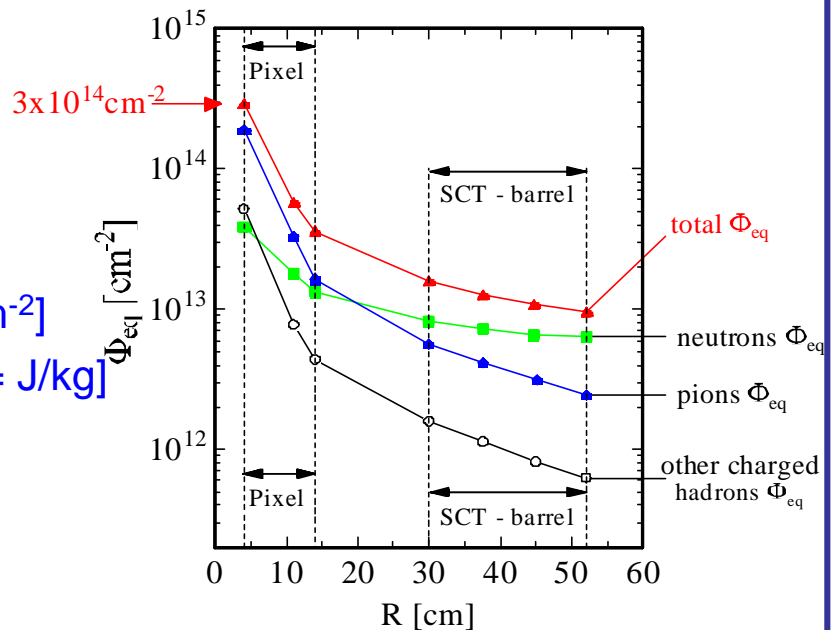
Radiation damage in silicon sensors

A major issue for LHC detectors !

Some definitions

- fluence: $\Phi = N/A$ [cm^{-2}]
- dose: $D = E/m$ [$\text{Gy} = \text{J/kg}$]

ATLAS - Inner Detector



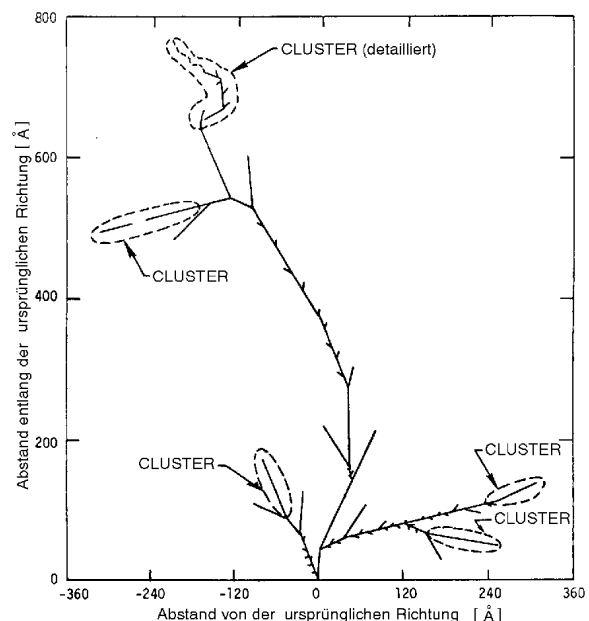
However: Specification of absorbed dose / fluence is not sufficient. Damage depends both on particle type (e, π, n, γ, \dots) and energy !

Many effects and parameters involved (not all well understood)!

Damage caused by
Non Ionising Energy Loss

Bulk effects: Lattice damage, vacancies and interstitials.

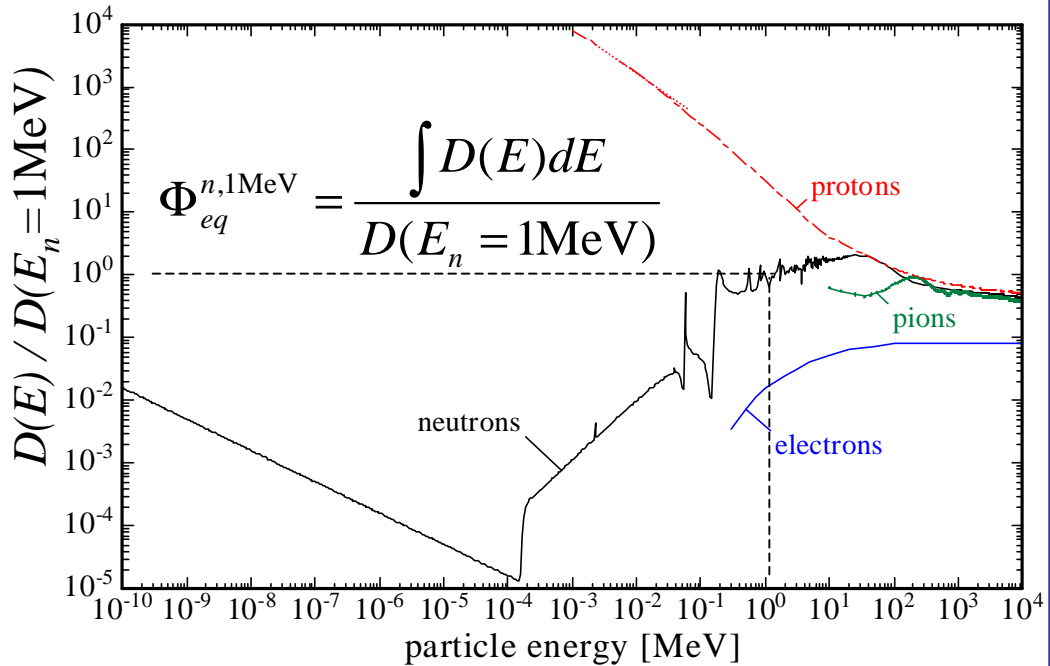
Surface effects: Oxide trap charges, interface traps.



NIEL hypothesis (not fully valid !):

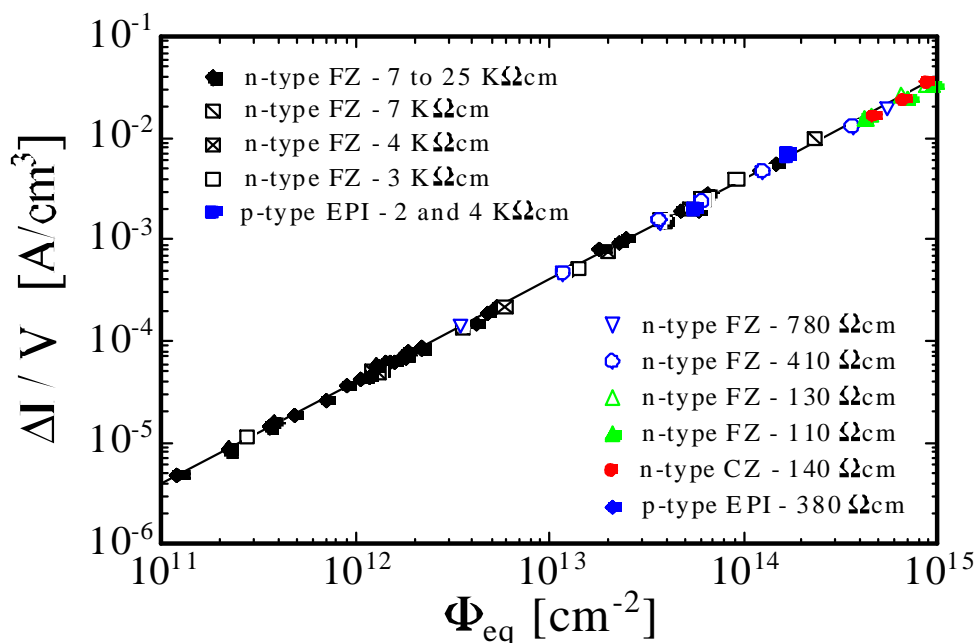
damage \propto energy deposition in displacing collisions

Rel. damage function
(normalized to neutrons of 1 MeV)

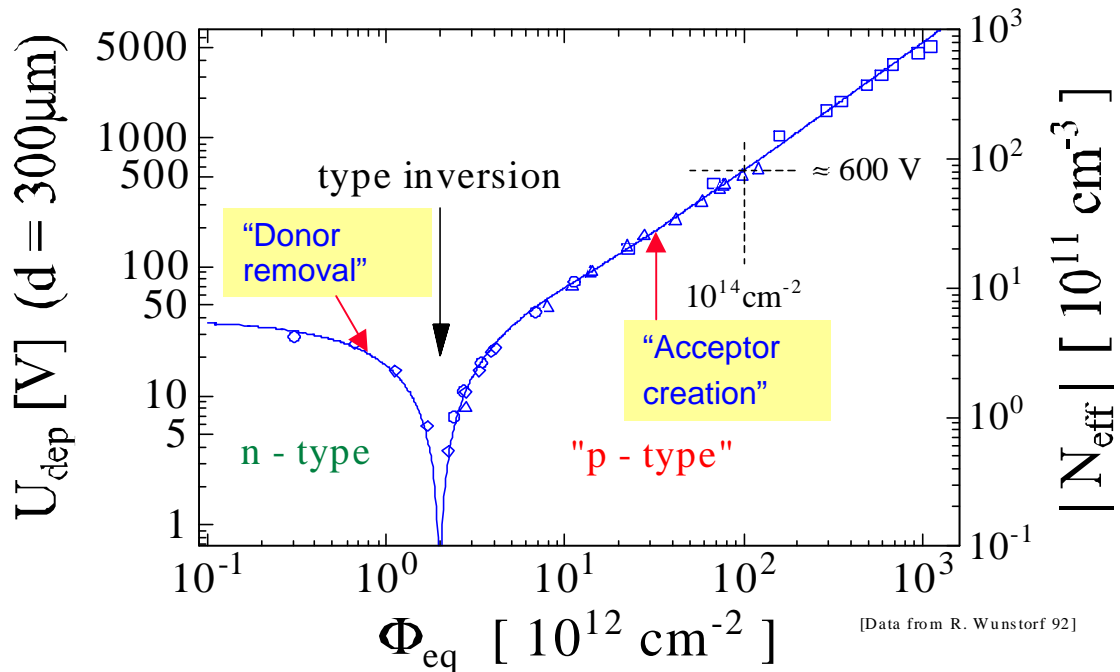


Main radiation induced macroscopic changes:

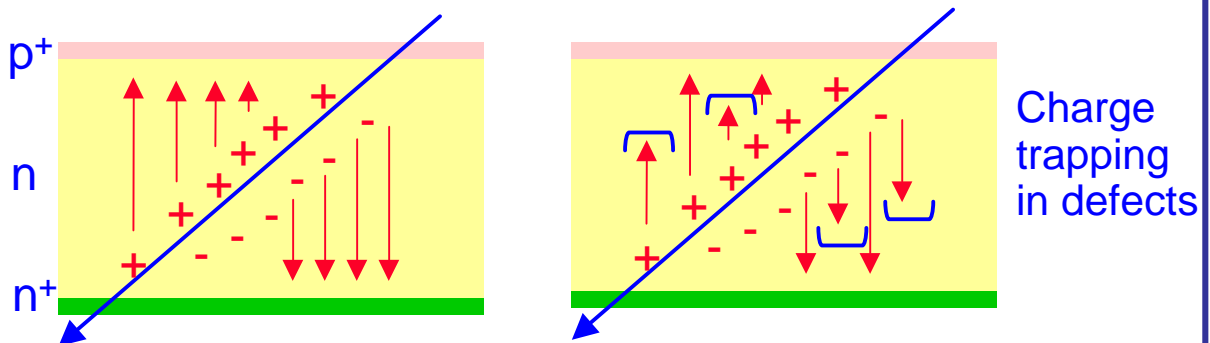
1. Increase of sensor leakage current



2. Change of depletion voltage. Very problematic.



3. Decrease of the charge collection efficiency



How to cope with the radiation damage ?

Possible strategies:

- **Geometrical:** build sensors such that they stand high depletion voltage (500V)
 - **Environmental:** keep sensors at low temperature ($\approx -10^\circ\text{C}$).
- Slower reverse annealing. Lower leakage current.

More advanced methods

- **Defect engineering.**



ROSE / RD48
<http://cern.ch/rd48>

Introduce specific impurities in silicon, to influence defect formation. Example Oxygen.

Diffusion Float Zone Oxygenated (DOFZ) silicon used in ATLAS pixel detector. Gain a factor 3.

- **Cool detectors to cryogenic temperatures**

(optimum around 130 k)

“zero” leakage current, good charge collection (70%) for heavily irradiated detectors ($1 \cdot 10^{15}$ n/cm²). **“Lazarus effect”**

RD39
<http://cern.ch/rd39>

- **New materials**

Diamond. Grown by Chemical Vapor Deposition. Very large bandgap (≈ 6 eV). No doping and depletion required! Material is still rather expensive. Still more R&D needed.

RD42
<http://cern.ch/rd42>

- **New detector concepts**

“3D detectors” → “horizontal” biasing
 faster charge collection
 but difficult fabrication process

